Available online at www.sciencedirect.com
ScienceDirect
Dyes and Pigments 77 (2008) 53–58
DYES and PIGMENTS
www.elsevier.com/locate/dyepig

Effect of synthesis parameters on a hematite–silica red pigment obtained using a coprecipitation route

M. Hosseini-Zori [a], F. Bondioli [b,*], T. Manfredini [b], E. Taheri-Nassaj [a]

[a] *Department of Materials Science and Engineering, Tarbiat Modares University, P.O. Box 14115-143, Tehran, Iran*
[b] *Dipartimento di Ingegneria dei Materiali e dell'Ambiente, Faculty of Engineering, Università di Modena e Reggio Emilia, Via Vignolese 905, 41100 Modena, Italy*

Received 9 November 2006; received in revised form 13 March 2007; accepted 17 March 2007
Available online 4 April 2007

Abstract

The morphology and the dimensions of the hematite particle influenced the shade of the red pigments obtained; both fine (<30 nm in length) spherical and long (>250 nm in length) acicular shapes gave poor red shades. The morphology of the hematite particles depends on the precipitant used; ammonia provided spherical, whereas NaOH produced acicular hematite particles. The dimensions of the hematite particles depended on the mineralisers used; while the silica structure did not influence pigment shade, the use of mineralisers promotes tridymite structure crystallization.

Keywords: Ceramic; Inclusion pigment; Non-toxic red pigment; Hematite–silica

1. Introduction

Inorganic natural and synthetic pigments produced and marketed as fine powders are an integral part of many decorative and protective coatings and are used for the mass coloration of many materials, including glazes, ceramic bodies and porcelain enamels. In these applications, the pigments disperse in the media, forming a heterogeneous mixture. The powders used to color ceramics must possess thermal and chemical stability at high temperature and must be inert to the action of molten glass (frits or sintering aids) [1]; these characteristics limit the number of available ceramic pigments [2–12]. The need for high chemical and thermal stabilities has dominated research and development in recent years, especially as regards new red or pink pigments. In particular, interest has focused on the development of inclusion pigments which are not tolerant of the high thermal and chemical environment, but which can be occluded in a stable glassy or crystalline matrix (heteromorphic pigments). The inclusion or encapsulation of a reactive, coloured or toxic crystal inside a stable crystalline or amorphous uncoloured matrix, provides protection to the chromophore; in this way, the crystal is inactivated inside the matrix.

Hematite–silica, heteromorphic pigments are popular despite the fact that the traditional preparation method yields powders that are unable to tolerate neither the glazing composition nor the sintering temperature. To achieve high-efficiency chromophore encapsulation, the temperature of the matrix sintering and crystallization must synchronize with the temperature of nucleation and growth of the occluded chromophore phase. The crystallization, sintering and inclusion processes must take place simultaneously and, consequently, control of the particle size and the choice of mineraliser are major parameters that need to be controlled [6].

In this work, a coprecipitation route, employing two precipitant agents, ammonia and sodium hydroxide, was used to include hematite in a silica matrix so as to control the microstructural

* Corresponding author.
E-mail address: bondioli.federica@unimore.it (F. Bondioli).

0143-7208/$ - see front matter © 2007 Elsevier Ltd. All rights reserved.
doi:10.1016/j.dyepig.2007.03.006

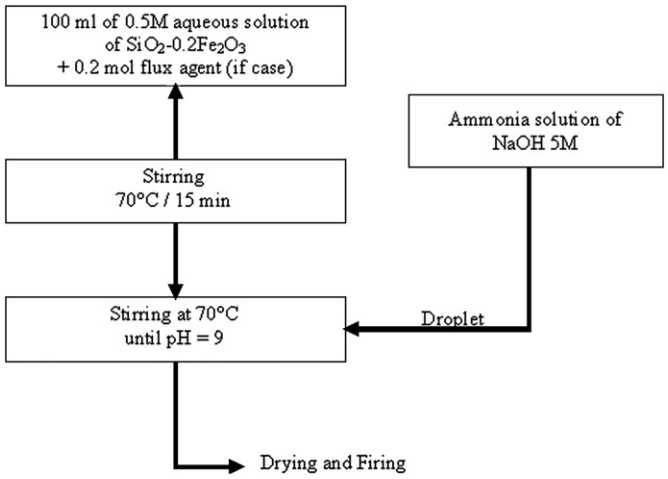

Fig. 1. Flux diagram of coprecipitation method used.

characteristics and particle morphology [1,3,6]. The effect of the mineralisers, NaF and NaCl, was investigated in order to optimize the pigment calcination temperature and secure control over the color obtained in an industrial glaze.

2. Experimental procedure

Samples of SiO_2–$0.2Fe_2O_3$ were prepared using the coprecipitation (P) route shown in Fig. 1. A 0.5 M aq solution was prepared by adding iron sulphate ($Fe_2SO_4 \cdot 7H_2O$, Aldrich) in the required mole ratio to an aqueous suspension of colloidal silica (Ludox). The precursors used are reported in Table 1. In mineralized samples, 0.2 M NaF, NaCl, NaF·NaCl or NaF·2NaCl (Sigma–Aldrich) was added to the aqueous solutions before reaction. Drops of concentrated ammonia solution (PI) or 5 M aq sodium hydroxide solution (PII) were then added to the mixture, which was continuously stirred and kept at 70 °C until the pH stabilized at 9. The resulting dark green coprecipitate was dried at 110 °C and fired. In order to determine the effects of firing temperature and mineraliser composition, the powders were fired at temperatures ranging from 800 to 1100 °C in an electrical furnace with a soaking time of 3 h. The fired samples were micronised, wet milled in water and finally dried at 110 °C.

To identify the crystalline phases present in the raw and fired samples, X-ray diffraction patterns were collected using a conventional powder technique in a Siemens Diffractometer (D500 mod) employing Cu Kα Ni-filtered radiation. To define the color developed by the samples, a Gretag Macbeth, *Color-Eye 7000*, was used, employing a 10° Standard Observer. The powder's microstructure was characterised using scanning electron microscopy (Philips XL-30) and by transmission electron microscopy (Jeol JEM 2010 equipped with a GIF Multiscan Camera 794).

Table 1
Precursors used to prepare $0.2Fe_2O_3$–SiO_2 samples

Sample	Method	Si precursor, Fe precursor and precipitant agent
PI	Coprecipitation	Ludox (30% in SiO_2), $FeSO_4 \cdot 7H_2O$ and NH_4OH
PII	Coprecipitation	Ludox (30% in SiO_2), $FeSO_4 \cdot 7H_2O$ and NaOH

Table 2
Crystalline phases and CIELab values of PI samples as a function of calcination temperature

Mineraliser	T (°C)	Phase composition (XRD)	Color $L^*/a^*/b^*$
Without	Raw	Ma	Maroon
	900	H	45.8/27.2/23.4
	1000	H, C(w)	43.5/26.6/23.1
	1100	H, C(s)	41.9/25.6/22.8
NaF	Raw	Ma	Green-yellow
	900	H, C(w)	45.1/26.2/21.3
	1000	H, C, T(w)	43.0/25.2/20.1
	1100	Local melting H, C(w), T_m	Brown
NaCl	Raw	Ma	Green-yellow
	900	H, C(w)	44.9/26.5/21.1
	1000	H, C(w), T	42.5/25.7/19.4
	1100	Local melting, H, T_m	Brown
NaF·NaCl	Raw	Ma, N(w), S, T_H	Light green
	800	N(w), H, T_m(w)	46.4/26.6/22.1
	900	N(w), H, T_m(s)	44.8/25.2/20.3
	1000	Local melting, H, T_m	Brown
NaF·2NaCl	Raw	Ma, N, S, T_H	Brown
	800	N(w), H, T_m	43.2/28.9/24.1
	900	N(w), H, T_m(s)	44.2/28.6/23.1
	1000	Local melting, H, T_m	Brown

Ma: $(NH_4)_2SO_4$ (mascagnite 00-001-0363); H: hematite (00-033-0664); C: cristobalite (01-076-0937); N: Na_2SO_4 (01-075-1979); T_m: tridymite-monoclinic (01-071-0197); T_h: tridymite-hexagonal (01-089-3141); S: NH_4Cl (00-001-1037); w: weak; s: strong.

Table 3
Crystalline phases and CIELab values of PII samples as a function of calcination temperature

Mineraliser	T (°C)	Phase composition (XRD)	Color $L^*/a^*/b^*$
Without	Raw	N	Dark brown
	900	N, H, C(w)	42.9/28.9/24.9
	1000	N, H, C(s)	41.7/27.9/19.8
	1100	Local melting, H, C	Red brown
NaF	Raw	N	Green
	900	N, H, T_o(w)	43.9/27.1/21.5
	1000	N, H, T_o(s), C(w)	42.7/25.8/21.6
	1100	Melting, H, T_o(w)	Brown
NaCl	Raw	N	Green-yellow
	900	N, H, T_o(w)	44.4/27.5/20.9
	1000	N, H, T_o(s), C(w)	43.0/26.2/19.7
	1100	Melting, H, T_o(w)	Brown
NaF·NaCl	Raw	F, N	Yellow-brown
	800	N, H, T_o(w)	46.1/26.5/19.8
	900	N, H, T_o(s), C(w)	43.6/25.9/18.6
	1000	Local melting, H, T_o	Brown
NaF·2NaCl	Raw	F, N, NaCl(w)	Light brown
	800	N, H, T_o(s), C(w)	45.9/26.9/24.2
	900	Local melting, H, To	52.8/26.3/23.1
	1000	Melting, H, T_o(w)	Brown

N: Na_2SO_4 (01-075-1979); H: hematite (00-033-0664); C: cristobalite-tetragonal (01-076-0937); T_o: tridymite-orthorhombic (00-002-0242); F: FeOOH (00-034-1266); w: weak; s: strong.

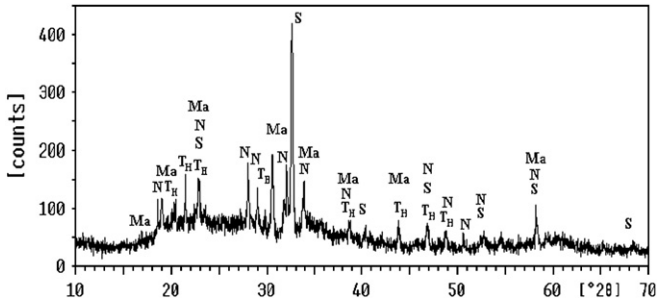

Fig. 2. XRD patterns of PI dried powder sample with NaF·NaCl mineraliser; Ma: $(NH_4)_2SO_4$, N: Na_2SO_4, T_h: tridymite-hexagonal, S: NH_4Cl.

3. Results and discussion

3.1. Thermal evolution of crystalline phases by XRD analysis

The main reactions involved in the coprecipitation route are [13]

$$FeSO_4 + 2NH_4OH \rightarrow (NH_4)_2SO_4 + Fe(OH)_2$$

$$FeSO_4 + 2NaOH \rightarrow Na_2SO_4 + Fe(OH)_2$$

$$Fe(OH)_2 \rightarrow FeOOH + H_2O$$

Moreover, when ammonia is the precipitant agent, other competitive reactions are present when both NaF and NaCl are used as mineralisers:

$$NaCl + NH_4OH \rightarrow NH_4Cl + NaOH \text{ and/or}$$

$$6NaCl + 2FeSO_4 \rightarrow 3Na_2SO_4 + 2FeCl_3$$

$$FeCl_3 + 3NH_4OH \rightarrow 3NH_4Cl + Fe(OH)_3$$

The XRD results and colorimetric data of the synthesized powders are reported in Tables 2 and 3. In the case of the uncalcined PI powders, the presence of ammonium sulphate can be attributed to the precipitant used in accordance with the reaction scheme reported above. Moreover, there were no peaks that could be attributed to FeOOH or silica precursor, probably due to the production of very fine or amorphous FeOOH that could be detected by XRD. In terms of the calcined PI powders, the use of mineralisers affected silica crystallization

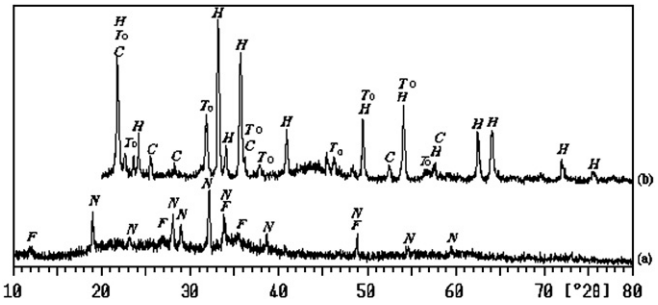

Fig. 3. XRD patterns of PII sample with NaF·NaCl mineraliser: (a) raw powders and (b) powders fired at 900 °C/3 h, N: Na_2SO_4, F: FeOOH, H; hematite, C: cristobalite-tetragonal, T_o: tridymite-orthorhombic.

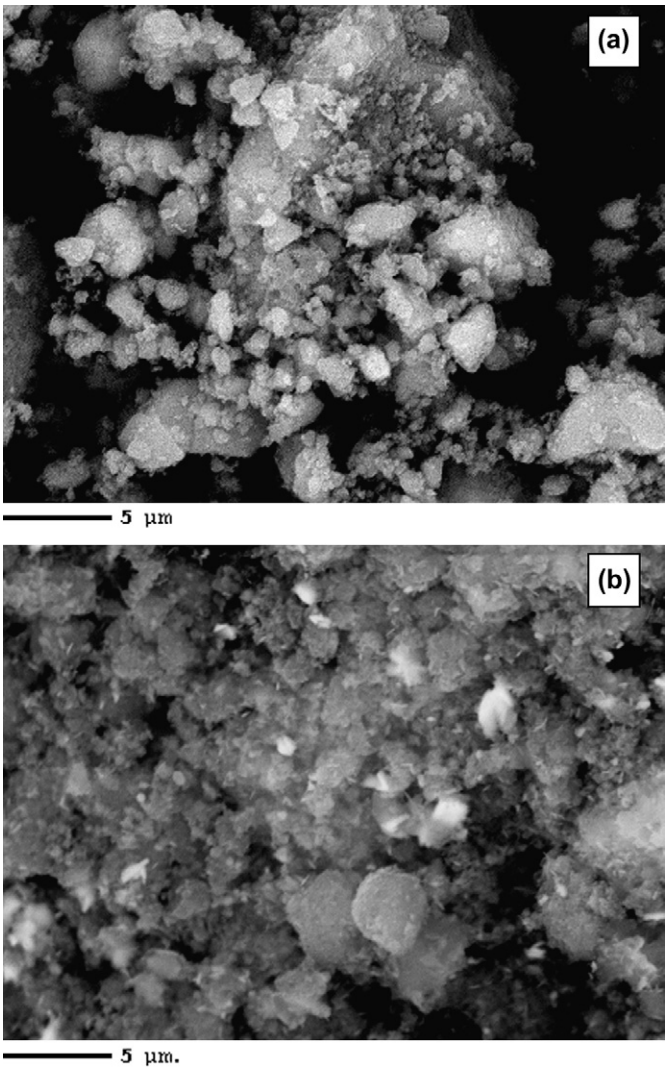

Fig. 4. SEM micrographs of PI (a) and PII (b) unfluxed samples fired at 1000 °C/3 h.

and promoted tridymite phase formation rather than cristobalite. Specifically, the use of two mineralisers allowed the crystallization of tridymite crystals even in dried powders (Fig. 2) although the crystalline structure changed on heating from hexagonal to monoclinic. In the context of the colorimetric data, a stronger red shade was obtained using two mineralisers, especially in the ratio NaF:2NaCl at a calcination temperature as low as 800 °C, as shown by the higher a^* value of 28.9. At higher temperature (1000 °C), the use of two mineralisers permitted local melting of the silica matrix due to the formation of eutectic compounds.

The results in Table 3 for the uncalcined, PII powders, showed sodium sulphates (Table 3) as the main crystalline phase; FeOOH crystals were only observed in samples obtained using both mineralisers (Fig. 3). As far as the calcined powders were concerned, the use of mineralisers promoted tridymite crystallization but in an orthorhombic structure. A red shade was obtained for powders obtained with or without a single mineraliser. Comparing the colorimetric and XRD data, FeOOH crystallization in the dried powder can be correlated

to a paler red shade of the pigments. In fact, during heat treatment, the FeOOH crystals could break down into larger hematite crystals, thus reducing encapsulation efficiency.

3.2. Microstructual analysis of samples using SEM and TEM techniques

Figs. 4 and 5 show the microstructures of the sample observed using SEM from which it is apparent that the unfluxed, fired samples comprised aggregates of micronic particles. Spherical amorphous silica particles, which were more homogeneous in size in PII (mean diameter of approximately 2 μm, Fig. 4b) than PI (Fig. 4a) and needle-like crystals of hematite are clearly visible. Fig. 5a shows the effect of NaF:NaCl as flux agent on PI samples fired at 1000 °C for 3 h. Large agglomerated particles are visible due to local melting [14]. Fig. 5b relates to PII with NaF as single flux agent: the micrograph shows low aggregation. When compared with Fig. 4b, Fig. 5b clearly shows that the mineraliser promoted the encapsulation of hematite crystals in the silica matrix, which lost its spherical morphology, which is a characteristic of an unfluxed sample.

The morphology of FeOOH and/or hematite particles can only be detected by TEM analysis. Fig. 6a shows the morphology of the precipitated particles; silica and iron oxide crystals of an acicular shape were observed. Fig. 6b, in contrast, demonstrates how the acicular hematite crystals were successfully occluded in the silica particles after firing. Moreover, the calcination step, as expected, promoted the growth of the hematite crystals, which, starting from 40 nm grew to approximately 100–150 nm in length. Iron oxide particles are acicular in

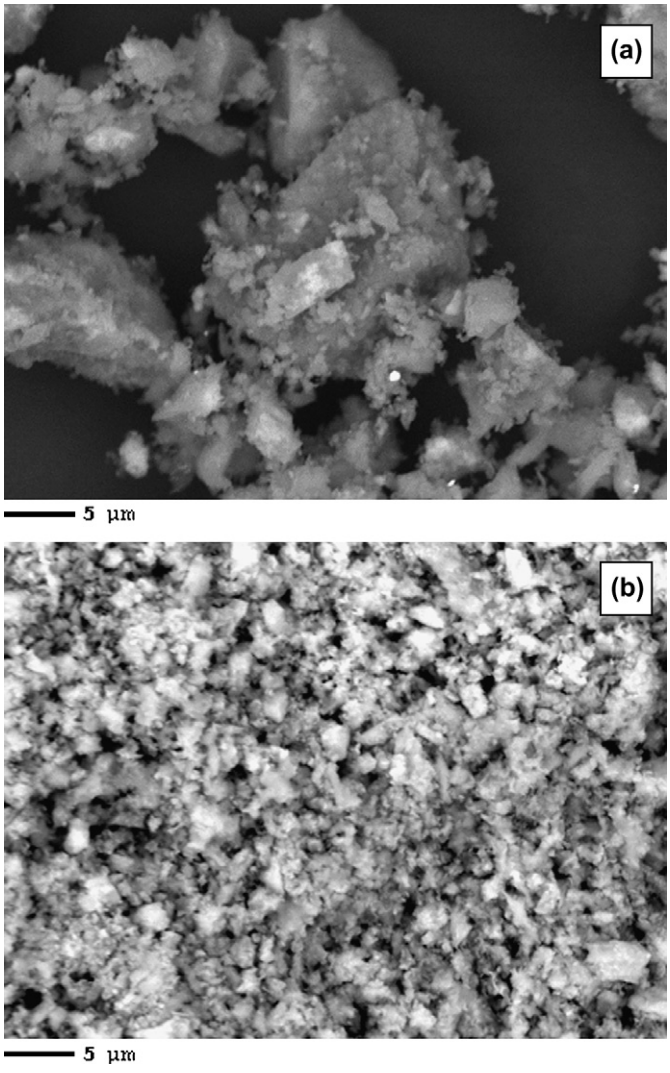

Fig. 5. SEM micrographs of PI sample with NaF·NaCl fired at 1000 °C/3 h (a) and PII sample with NaF fired at 1000 °C/3 h (b).

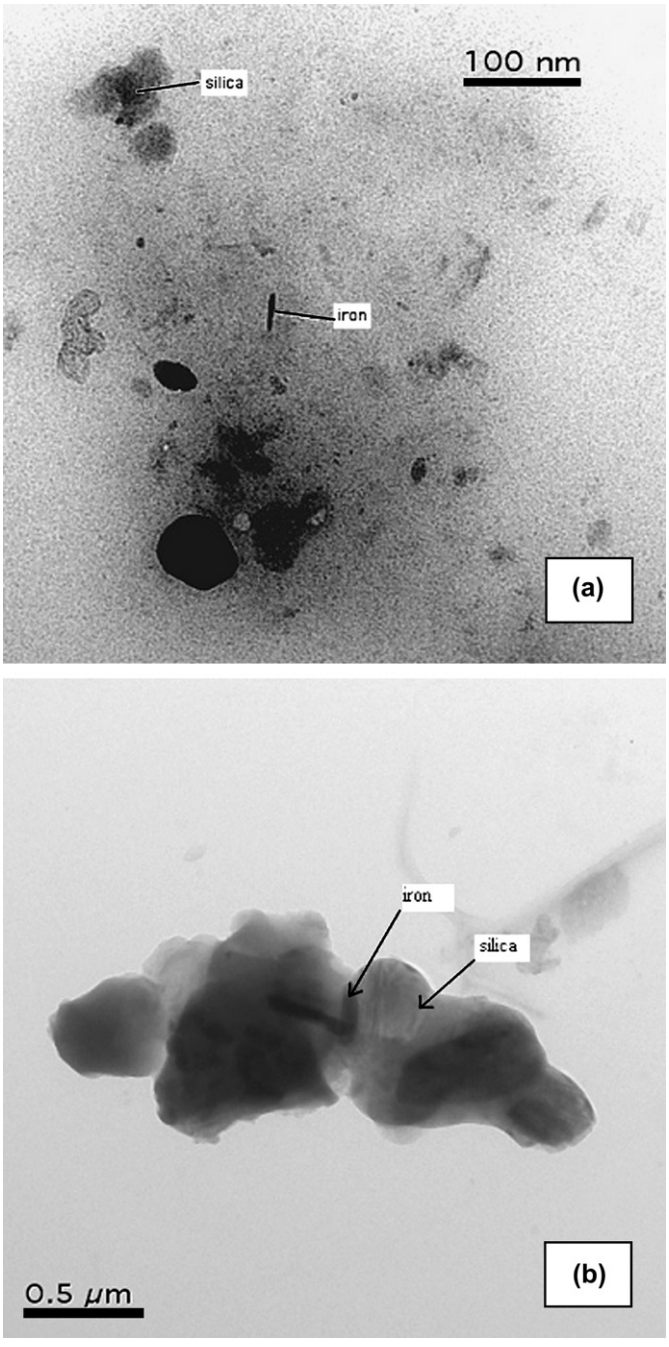

Fig. 6. TEM micrographs of unfluxed PII sample: (a) raw powder and (b) fired at 1000° C/3 h.

both raw and fired particles. It can therefore be concluded that the morphology of hematite is dependent on the morphology of the initial raw iron hydroxide. Fig. 7 indicates that the addition of the flux agent influenced the iron particle's growth with crystals being as long as 250 nm.

Fig. 8a shows the TEM images of the PI sample without mineraliser from which it is clear that the sample comprised very fine particles even after calcination at 1100 °C. In this case, the shape of the hematite particles was spherical with a diameter of approximately 20–30 nm. The use of one or both mineralisers did not change the spherical shape of the

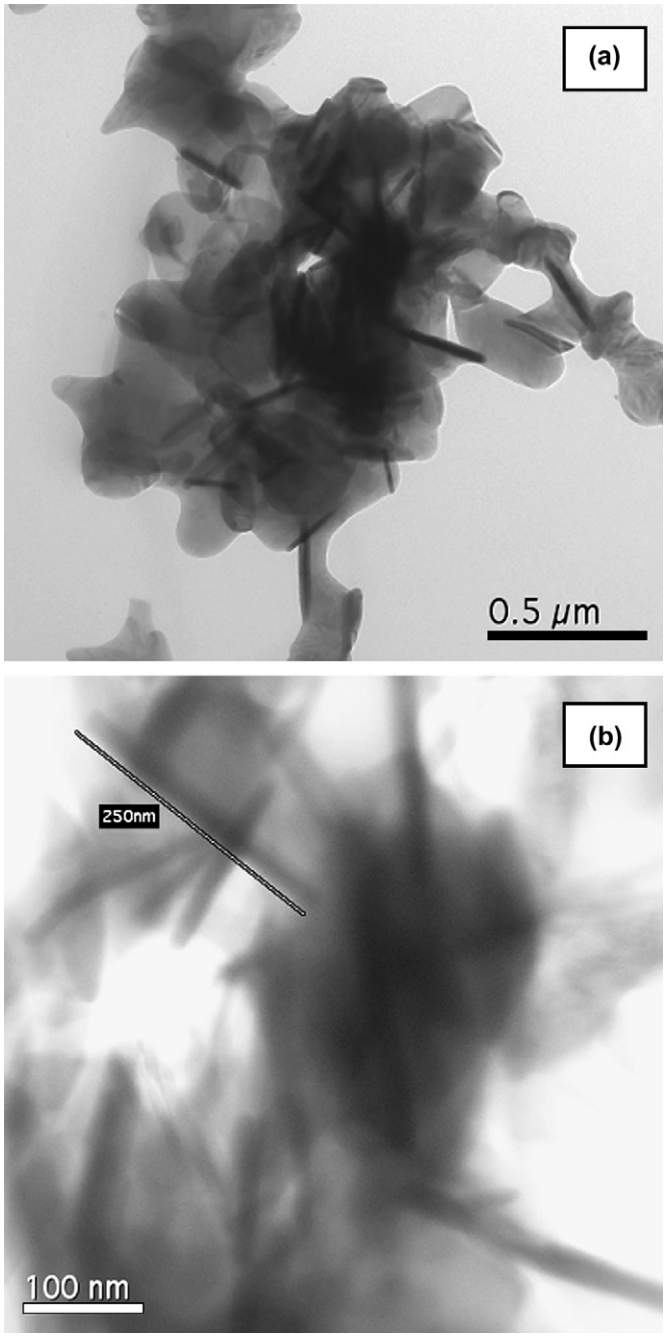

Fig. 7. TEM micrographs of PII sample with NaF fired at 1000 °C/3 h (b) particular.

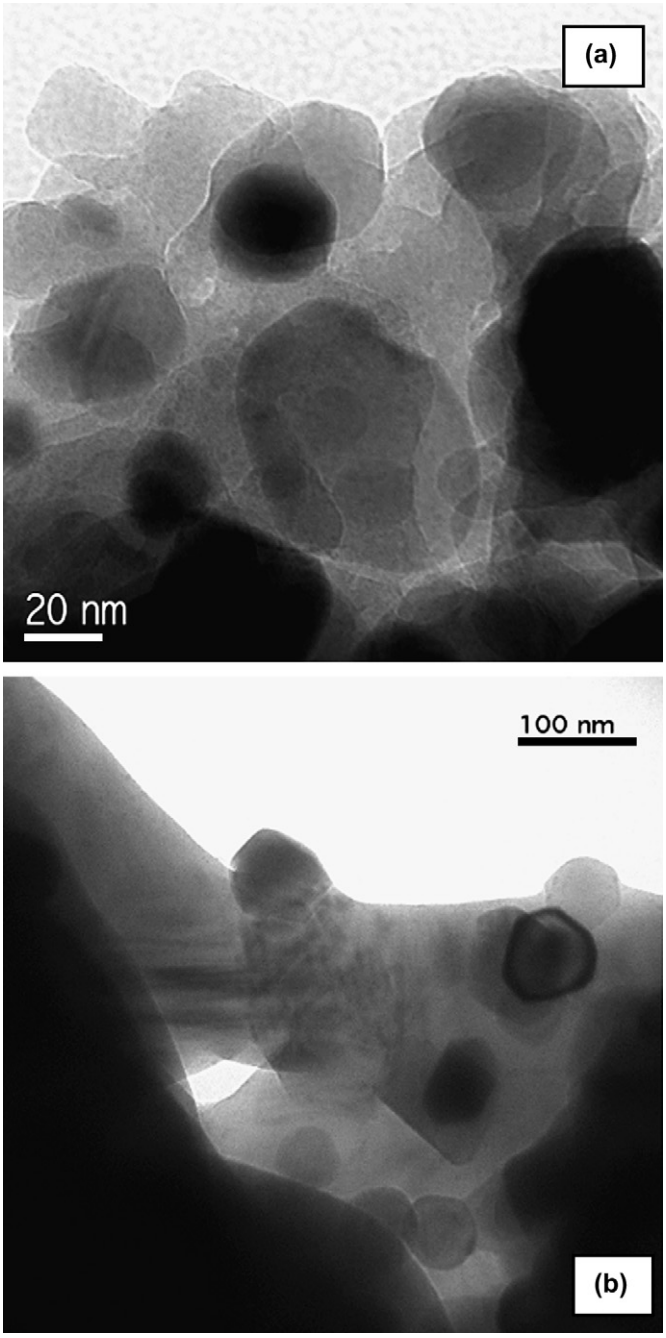

Fig. 8. TEM micrographs of PI powders: unfluxed fired at 1100 °C/3 h (a) and with NaF·2NaCl fired at 900 °C/3 h (b).

hematite crystals, but increased the diameter of the spherical particles up to approximately 60 nm (Fig. 8b). Correlating this evidence with the colorimetric data (Table 2) shows that the weak red shade of these powders can be attributed to the nanometric size and the shape of the hematite crystals [15].

4. Conclusions

The morphology and dimensions of the hematite particle directly effect the shade of the red pigments obtained; both fine (<30 nm in length) spherical and long (>250 nm in length) acicular shapes gave weak shades. The morphology

of the hematite particles depended on the precipitant used; ammonia provided spherical, whereas NaOH produced acicular hematite particles. The dimensions of the hematite particles depend on the mineralisers used; the silica structure does not influence shade although the use of mineralisers promotes tridymite structure crystallization.

Acknowledgements

We are grateful to Dr. Mauro Zapparoli and Dr. Massimo Tonelli for their kind help regarding TEM studies. Our thanks also go to Dr. Alireza Mirhabibi for his valuable advice.

References

[1] Vicent JB, Llusar M, Badenes J, Tena MA, Vicente M, Monros G. Occlusion of chromophore oxides by sol–gel methods: application to the synthesis of hematite–silica red pigments. Bol Soc Esp Ceram Vidrio 2000;39(1):83–93.

[2] Procyk B, Kucharski J, Stoch L. Ecological red pigments based on copper glass. Ind Ceram 1997;(926):342–4.

[3] Bondioli F, Ferrari AM, Leonelli C, Manfredini T. Synthesis of Fe_2O_3/silica red inorganic inclusion pigments for ceramic application. Mater Res Bull 1998;33(5):723–9.

[4] Llusar M, Badenes JA, Calbo J, Tena MA, Monros G. Environmental and colour optimisation of mineraliser addition in synthesis of iron zircon ceramic pigment. Br Ceram Trans 2000;99(1):14–22.

[5] Bondioli F, Manfredini T, Siligardi C, Ferrari AM. New glass–ceramic inclusion pigment. J Am Ceram Soc 2005;88(4):1070–1.

[6] Garcia A, Llusar M, Badenes J, Tena MA, Monros G. Encapsulation of hematite in zircon by microemulsion and sol–gel methods. J Sol-Gel Sci Technol 2003;27:267–75.

[7] Gualtieri AF. Natural red pigment for single-fired ceramic glaze. Am Ceram Soc Bull December 2000;48–52.

[8] Bondioli F, Manfredini T. The search for new red pigments. Am Ceram Soc Bull 2000;79(2):68–70.

[9] Jansen M, Letschert HP. Inorganic yellow-red pigments without toxic metals. Nature 2000;404(6781):980–2.

[10] Aruna ST, Ghosh S, Patil KC. Combustion synthesis and properties of $Ce_{1-x}Pr_xO_{2-\delta}$ red ceramic pigments. Int J Inorg Mater July 2001; 3(4–5):387–92.

[11] Baldi G, Dolen N. Synthesis of a new class of red pigments based on perovskite type lattice $A_xB(2-x-y)CrYO3$ with $x = 0.9–1.1$, $y = 0.05–0.12$, A = Y, lanthanides, B = Al for use in body stain and high temperature glazes. Effect of Cr+++ and metal A on the colour of ceramic pigment. Mater Eng 1999;10(2):151–64.

[12] Olazcuaga R, Le Flem G, Alarcon J. Introduction of Tb^{4+} into CeO_2 to obtain stable red pigments at high temperatures. Bol Soc Esp Ceram Vidrio 1993;32(5):307–10.

[13] Lewis PA. Pigment handbook, properties and economics. 2nd ed., vol. I. John Wiley & Sons; 1988. p. 287–9.

[14] Hiroaki K, Sridhar K. Role of alpha-Fe_2O_3 morphology on the color of red pigment for porcelain. J Am Ceram Soc 2003;86(1):183.

[15] Hosseini-Zori M, Taheri E, and Mirhabibi AR. Effective factors on synthesis of the hematite–silica red inclusion pigment. Ceram Int, accepted for publication.